

We are IntechOpen, the world's leading publisher of Open Access books Built by scientists, for scientists

5,800

Open access books available

142,000

International authors and editors

180M

Downloads

Our authors are among the

154

Countries delivered to

TOP 1%

most cited scientists

12.2%

Contributors from top 500 universities



WEB OF SCIENCE™

Selection of our books indexed in the Book Citation Index
in Web of Science™ Core Collection (BKCI)

Interested in publishing with us?
Contact book.department@intechopen.com

Numbers displayed above are based on latest data collected.
For more information visit www.intechopen.com



Reactive Distillation Applied to Biodiesel Production by Esterification: Simulation Studies

Guilherme Machado, Marcelo Castier, Monique dos Santos, Fábio Nishiyama, Donato Aranda, Lúcio Cardozo-Filho, Vladimir Cabral and Vilmar Steffen

Abstract

Reactive distillation is an operation that combines chemical reaction and separation in a single equipment, presenting various technical and economic benefits. In this chapter, an introduction to the reactive distillation process applied to the biodiesel industry was developed and complemented by case studies regarding the production of biodiesel through esterification a low-cost acid feedstock (corn distillers oil) and valorization of by-products (glycerol) through ketalization. The kinetic parameters of both reactions were estimated with an algorithm that performs the minimization of the quadratic differences between experimental and calculated data through a Nelder-Mead simplex method. A 4th order Runge Kutta method was employed to integrate the conversion or concentration equations used to describe the kinetics of the reactions in a batch reactor. Both processes were simulated in the commercial software Aspen Plus with the estimated kinetic parameters. The results obtained are promising and indicate that the productivity of both processes can be improved with the application of reactive distillation technologies. The simulated esterification process with an optimized column resulted in a fatty acids conversion increase of 84% in comparison to the values lower than 50% obtained in the experimental tests. Solketal production through ketalization also achieved a high glycerol conversion superior to 98%.

Keywords: reactive distillation, biodiesel, esterification, transesterification, simulation

1. Introduction

Reactive distillation is an operation that incorporates chemical reaction and physical separation in a single unit [1]. This process, when applicable, has several potential advantages for the industry when compared to conventional systems, such as the reduction of capital costs, improvement of component separations, use of fewer instruments for monitoring, reduction of energy costs, and improvement in reaction selectivity [2–6]. Among the possible applications of reactive distillation, the separation of azeotropic mixtures and compounds with similar boiling points can be carried out by adding a reagent that promotes the consumption of one component of the mixture and forms a product with markedly different physical

properties, thereby favoring separation. However, the use of reactive distillation is more frequent in systems where product formation is limited by chemical equilibrium. This separation technique allows for the constant removal of one or more products promotes or increases reactant conversion [7].

The first patents for the reactive distillation process were published in the 1920s, developed by Backhaus for the production of esters [8–10]. However, few industrial applications were developed before the 1980s [11], when the commercial process for methyl acetate synthesis via reactive distillation with a homogeneous catalyst was patented by Agreda and Partin [12], in collaboration with the Eastman Chemical Company. This application of reactive distillation is considered an exemplary case because of the substantial reduction in process costs ($\sim 80\%$) [13] achieved through the elimination of units, such as reactors and separation columns, and the possibility of heat integration. The conventional methyl acetate synthesis process (**Figure 1**), which comprises 11 different steps and 28 pieces of equipment, was replaced by only a highly integrated reactive distillation column (**Figure 2**), enabling the aforementioned reduction in process costs. Recent uses of reactive distillation in chemicals production such as acetic acid and methanol [14], alkyl carbonates [15], butadiene [16], butyl acetate [17], carboxylic acids and ether [18] and carboxylic esters [19] are described in patents.

Reactive separation conveniently combines the production and removal of one or more products, enabling improvements in reaction productivity and selectivity. However, despite the benefits of this process, the planning and control of reactive distillation columns are hindered by complex interactions between reaction and separation. Operation conditions resulting in the formation of equilibrium between liquid–liquid–vapor phases, low mass transfer rates between liquid and vapor phases or diffusion inside the catalyst (for heterogeneous reactions) and chemical kinetics with reduced reaction rate need to be avoided or minimized [20]. Additionally, since both separation and reaction take place simultaneously in the same unit, the temperatures and pressures required for the two steps must have similar values [21]. If the overlap of operating conditions is not significant, the use of reactive distillation is not recommended [2].

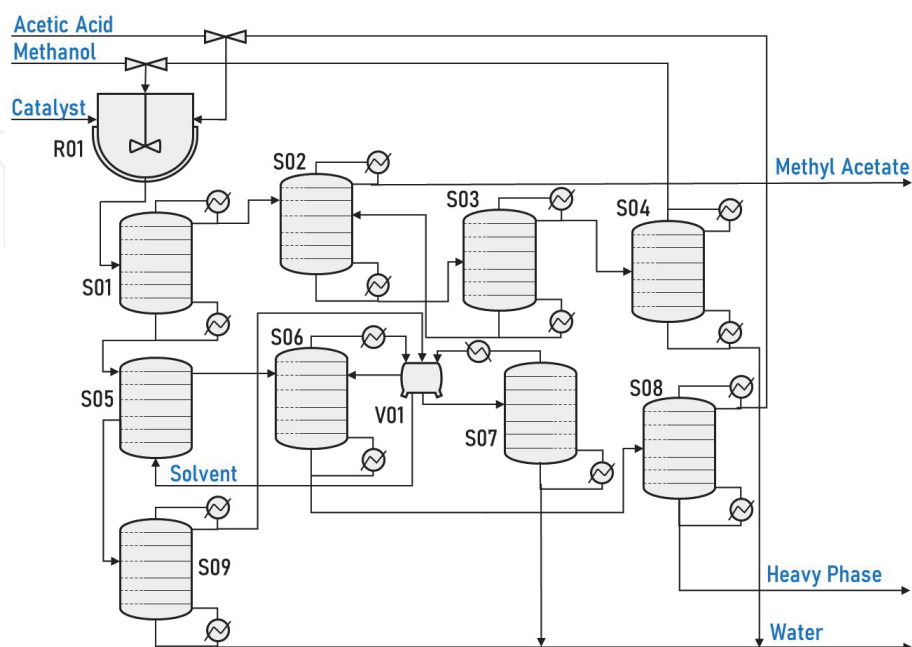


Figure 1.

Schematic representation of the conventional process for the synthesis of methyl acetate. Caption: R01: reactor; S01: mixer; S02: extractive distillation; S03: solvent recovery; S04: methanol recovery (MeOH); S05: extractor; S06: azeotropic column; S07–S09: flash columns; S08: acetic acid recovery; V01: decanter.

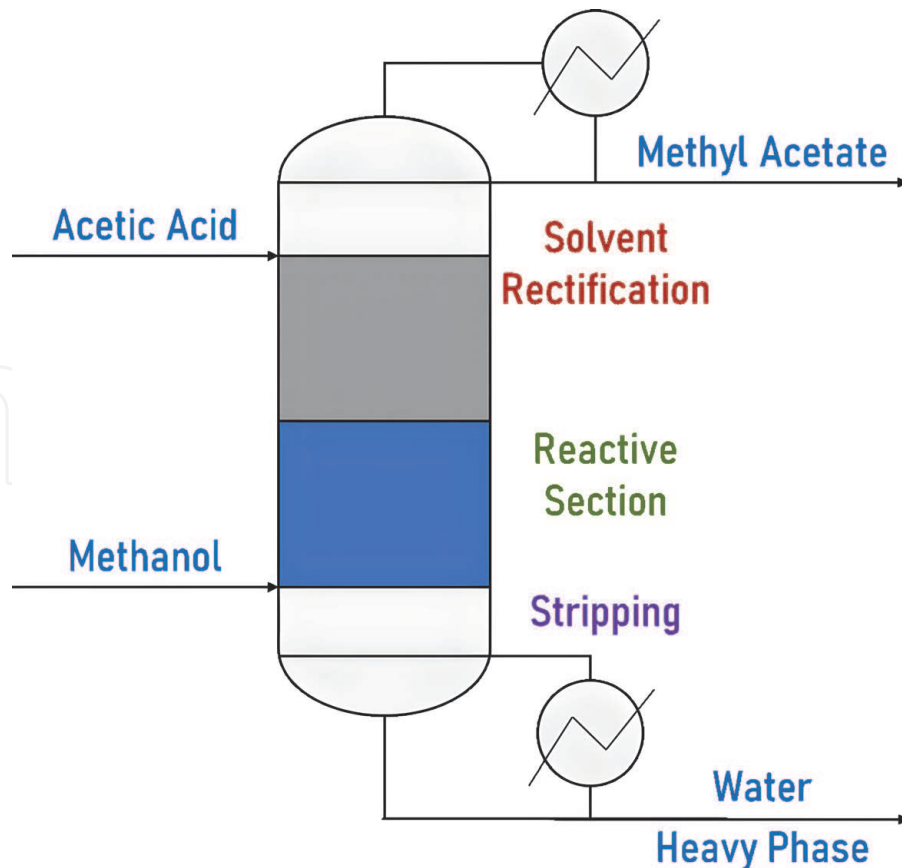


Figure 2.
 Schematic representation of the integrated process for the production of methyl acetate by reactive distillation.

2. Reactive distillation - biodiesel applications

The trend toward the use of biofuels has resulted from increased attention to topics related to mitigating environmental impacts by reducing the consumption of fossil fuels [22]. In this context, biodiesel is considered the main substitute fuel for diesel oil due to its lower polluting potential and the possibility of being used in diesel engines without the need for significant modifications [23, 24].

Biodiesel (alkyl esters) can be obtained by several reaction routes. The most conventional of them is the transesterification of triglycerides (oils) with short-chain alcohols (Eqs. (1)–(3)), such as methanol and ethanol, with homogeneous alkaline catalysts [25]. However, the raw material needed for this reaction must have reduced levels of acidity and moisture to avoid saponification reactions [26]. Due to the high costs of obtaining feedstocks that meet these specifications and competition with the food industry, studies aimed at the production of biodiesel from residual oils with a high content of fatty acids have been published [27–30].



One of the alternatives to reduce the typical acidity of residual oils is to carry out a previous fatty acid esterification step [25] (Eq. (4)). However, in this process, with reaction and separation occurring in different units, chemical equilibrium limits the yield because the reaction that forms one of the products, water is reversible [31].



Therefore, the use of a reactive distillation column can be justified and may result in higher fatty acid conversions compared to those achieved in conventional systems. **Tables 1** and **2** provide an overview of the literature on esterification and transesterification reactions aimed at producing biodiesel.

In general, the main objective of the evaluated studies on esterification in reactive distillation columns is to increase the yield of the biodiesel production process by shifting the chemical equilibrium of the reaction. However, for transesterification studies, reactive distillation systems are considered mainly due to the possible reduction in the reaction time or in the purification costs of the biodiesel alkyl esters formed. This difference in purpose presumably originates from the necessity of milder transesterification reaction conditions when compared to the esterification route for the attainment of high biodiesel yields.

3. Mathematical Modeling

Mathematical modeling of a reactive distillation column was developed in [51] with considerations described in [52]. In their study, the authors assume the absence of chemical equilibrium in the stages and steady-state operation, with reaction rates being explicitly considered in the model of each stage, Murphree separation efficiency equal to 100% and feeding performed by single-phase streams.

Such methodology, presented in this section, was used in the studies of the references [2, 38, 39,53]. The nomenclature for the terms used in the equations is described in **Table 3**.

Ref.	Feedstock	Catalyst	Temperature	Simulation software	FFA conv.
[31] ^a	Oleic acid	H ₂ SO ₄ (1–3 FFA wt%)	130–150°C	—	79.6%
[32] ^a	Dodecanoic acid	Solid acid catalyst (0–5 FFA wt%)	120–180°C	AspenOne 2004	~95.0%
[33] ^a	Dodecanoic acid	Metal oxides (0–10 FFA wt%)	120–180°C	AspenOne 2004	~72.0%
[34] ^a	Non-edible oil mixture	Tin (II) chloride (1–9 oil wt%)	40–60°C	Aspen Plus V8.8	78.3%
[35] ^b	Dodecanoic acid	Sulfated Zirconia	130°C (FFA feed)	Aspen Plus V9	99.9%
[36] ^a	Fatty acids mixture	Nb ₂ O ₅ (5 FFA wt%)	90–170°C	Aspen Plus V7.3	96.0%
[37] ^b	Fatty acids mixture	Sulfuric acid	417°C (FFA feed)	Aspen Plus	—
[38] ^b	Fatty acids	Solid acid catalysts	58, 145, 207°C (FFA feed)	Fortran Algorithm	>98.0%
[39] ^b	Hydrolyzed soybean oil	Niobium oxide	207°C (FFA feed)	Fortran Algorithm	>98.0%
[40] ^a	Fatty acids	Sulfuric acid (0.33–0.66 wt%)	50–70°C	Aspen Plus V10	~90.0%

^aExperimental tests performed by the authors.

^bNo experimental tests performed by the authors.

Table 1.
Reactive distillation studies aimed at the production of biodiesel through esterification.

Ref.	Feedstock	Catalyst	Temperature	Simulation software	Yield
[41] ^a	Soybean oil	NaOH (0.5–1.5 oil wt%)	50°C (oil feed)	—	98.2%
[42] ^a	Canola oil	KOH, KOCH ₃ (0.73–1.83 oil wt%)	100–160°C (reboiler)	—	94.9%
[43] ^a	Canola oil	KOH	95–150°C (reboiler)	—	94.4%
[44] ^a	Cooking oil	12-Tungstophosphoric acid hydrate	20–30°C (oil feed)	—	93.8%
[45] ^a	Palm oil	KOH (0.5–2 oil wt%)	85–120°C (reboiler)	—	92.3%
[46] ^b	Triolein	NaOH	55°C (oil feed)	CHEMCAD/MATLAB	90.3%
[47] ^b	Soybean oil	NaOH	25–90°C (oil feed)	HYSYS	~97.0%
[48] ^b	Algal oil	H ₂ SO ₄	<150°C (reboiler)	MATLAB	—
[49] ^b	Trilinolein	NaOH/ Magnesium methoxide	60–150°C (column)	Aspen Plus	98.3%
[50] ^b	Soybean oil	NaOH/CaO + Al ₂ O ₃	60°C/25°C	Aspen Plus V8.4	—

^aExperimental tests performed by the authors.

^bNo experimental tests performed by the authors.

Table 2.
 Reactive distillation studies aimed at the production of biodiesel through transesterification.

Symbol	Description
$C_{i,j}$	Molar concentration
$C_{p,i}^L$	Molar specific heat in the liquid phase
E_j	Relationship between vapor and liquid streams
$F_{i,j}$	Feed molar flow
$f_{i,j}^{eq}$	Phase equilibrium function
$f_{i,j}^m$	Mass balance function
f_j^{vl}	Function that correlates liquid and vapor streams
$f_{k,j}^r$	Reaction rate function
H_j^I	Total enthalpy of the vapor stream
H_j^{II}	Total enthalpy of the liquid stream
$k_{k,j}$	Kinetic reaction constant
$n_{i,j}^I$	Molar flow of vapor
$n_{i,j}^{II}$	Molar flow of liquid
nc	Number of components
nr	Number of chemical reactions
$P_{i,j}^{sat}$	Liquid saturation pressure
P_j	Pressure
Q_j	Heat added or removed
R	Universal gas constant
R_j	Liquid withdrawal fraction
T_j	Temperature
T_{ref}	Reference temperature (298.15 K)

Symbol	Description
v_j^{II}	Liquid molar volume of pure compound
$x_{i,j}^{\text{I}}$	Molar fraction in vapor phase
$x_{i,j}^{\text{II}}$	Molar fraction in liquid phase
Z_j	Lateral vapor withdrawal fraction
$\alpha_{i,k}$	Kinetic order of reaction
Δh_i^{vap}	Molar enthalpy of vaporization
$\gamma_{i,j}^{\text{vap}}$	Activity coefficient in the liquid phase
$\nu_{i,k}$	Stoichiometric coefficient
$\xi_{k,j}$	Reaction rate

(references: i = component, j = column stage, k = reaction).

Table 3.
Nomenclature of terms used in mathematical modeling.

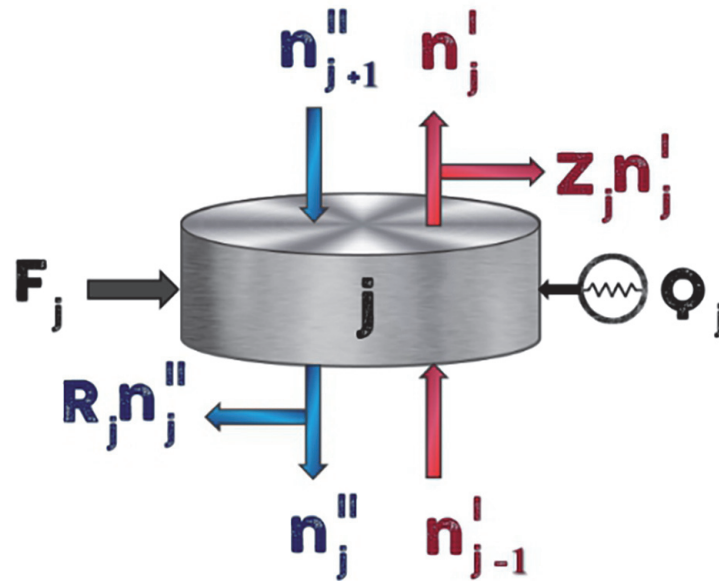


Figure 3.
Configuration of each stage j in the reactive distillation column. Source: [53].

The generic plate scheme adopted by the authors is represented in **Figure 3**.

Eq. (5), which represents the mass balance of component i in stage j of the column as a residual function, is given by:

$$f_{i,j}^m = (R_j + 1)n_{i,j}^{\text{II}} + (Z_j + 1)n_{i,j}^{\text{I}} - \left(n_{i,j+1}^{\text{II}} + n_{i,j-1}^{\text{I}} + F_{i,j} + \sum_{k=1}^{nr} \nu_{i,j} \xi_{k,j} \right) = 0 \quad (5)$$

Assuming that the streams that leave the stage are in phase equilibrium, Eq. (6) relates the mole fractions in the liquid and vapor phases:

$$f_{i,j}^{eq} = \ln \left(x_{i,j}^{\text{I}} P_j \right) - \ln \left(x_{i,j}^{\text{II}} \gamma_{i,j}^{\text{II}} P_{i,j}^{\text{sat}} \right) = 0 \quad (6)$$

In this expression, the Poynting correction and the fugacity coefficient of the pure saturated compounds are neglected. In addition, and the vapor phase is considered to be an ideal gas mixture as a consequence of the

assumption that the column operates at low pressure, close to atmospheric conditions.

The equation for the rate of reaction k in stage j is represented by Eq. (7), which can be expressed as a residual equation by applying the logarithm function (Eq. (8)).

$$\xi_{k,j} = k_{k,j} \prod_{i=1}^{nc} C_{i,j}^{\alpha_{i,k}} \quad (7)$$

$$f_{k,j}^r = \ln k_{k,j} + \sum_i^{nc} \alpha_{i,k} \ln \left(\frac{x_{i,j}^H}{v_j^H} \right) - \ln \xi_{k,j} = 0 \quad (8)$$

Assuming that the molar volume of the liquid phase is that of an ideal solution and describing Eq. (8) as a function of the activity coefficients of the components in the liquid phase, Eq. (9) is obtained.

$$f_{k,j}^r = \ln(k_{k,j}) + \sum_i^{nc} \alpha_{i,k} \ln(x_{i,j}^H + \gamma_{i,j}^H) - \ln(\xi_{k,j}) = 0 \quad (9)$$

Eq. (10), which describes the energy balance of stage j , is needed to calculate the temperature, which is different at each stage of the reactive distillation column. Positive and negative values of Q_j correspond to the heat being supplied to or removed from the column, respectively.

$$f_j^h = (R_j + 1)H_j^H + (Z_j + 1)H_j^L - (H_{j+1}^H + H_{j-1}^L + H_{F_j} + Q_j) = 0 \quad (10)$$

The ratio between the molar flows of vapor and liquid leaving each stage of the column is represented using Eq. (11). This equation is intended to make the condenser and reboiler specifications more flexible by associating the relationship between the liquid and vapor streams that leave the column stages.

$$E_j = \frac{(Z_j + 1) \sum_{i=1}^{nc} n_{i,j}^L}{(R_j + 1) \sum_{i=1}^{nc} n_{i,j}^H} \quad (11)$$

When written in the residual form, as in Eq. (12), the equation has the following form:

$$f_j^{vl} = (Z_j + 1) \sum_{i=1}^{nc} n_{i,j}^L - E_j (R_j + 1) \sum_{i=1}^{nc} n_{i,j}^H = 0 \quad (12)$$

The values of the E_j parameter for each form of operation of the condenser and reboiler (partial or total) are shown in **Table 4**.

In the study developed by [2, 36, 37, 48], all cases of simulated reactive distillation column configurations used a partial reboiler and total condenser ($E_1 \neq 0$ and $E_N = 0$).

Solving the set of equations that describe a reactive distillation column is an arduous task, and rigorous mathematical models aimed at a computer simulation of this type of equipment were not developed until the 1970s [54].

Reboiler (stage 1)		Condenser (stage N)	
Partial	Total	Partial	Total
$Z_1 = 0$	$Z_1 \neq 0$	$Z_N = 0$	$Z_N = 0$
$R_1 = 0$	$R_1 = 0$	$R_N = 0$	$R_N \neq 0$
$E_1 \neq 0$	$E_1 \rightarrow \infty$	$E_N \neq 0$	$E_N = 0$

Table 4.
Characteristics of column heaters (reboiler and condenser).

In recent decades, commercial software that has specific models and algorithms for reactive distillation operations has been widely used, as shown previously in **Tables 1** and **2**. The simulations developed in the subsequent section, referring to case studies applied to biodiesel production and co-product valuation, use the RADFRAC module present in the commercial Aspen Plus software, which solves the equations of mass balance, energy balance, phase equilibrium and the sum of molar fractions (MESH) [55] through the “inside-out” algorithm [54].

4. Fatty acid esterification simulation

4.1 Methodology

4.1.1 Kinetic parameters estimation

The kinetic parameters for the esterification of fatty acids (FFA) present in corn distillers oil from DDGS (dried distillers grains with solubles) were estimated by a model fitting of the FFA conversion data (**Table 5**) obtained by our group. The reaction (Eq. (13)) was carried out at the temperatures of 150, 175 and 200°C, with ethanol and NbOPO₄ (catalyst), following a molar alcohol:FFA ratio of 10:1 and catalyst load of 10% (FFA mass).

The methodology applied aims to estimate the pre-exponential factor (k_0) and the activation energy (E_a) of the reaction. To fit the kinetic parameters, the objective function to be minimized is the squared difference between the experimental values of the FFA conversion and those calculated with a reversible pseudo-homogeneous model (Eq. (14)). The reaction rate (r_F) equation was applied to Eq. (15), which describes a batch reactor in terms of the FFA conversion (x) in a given time (t).

A Nelder–Mead [56] simplex algorithm and a 4th order Runge–Kutta [57] method were used to perform the objective function minimization and conversion equation integration steps, respectively. The reaction rate (r_F) was obtained through the model and the specific reaction rate constants k (L/mol.s) were expressed by the Arrhenius equation (Eq. (16)). Through this methodology, the parameters E_a and k_0 for the reaction rate constants of the forward and reverse esterification reactions were estimated.



$$-r_F = k_1 C_F C_A - k_2 C_E C_W \quad (14)$$

$$\frac{dx}{dt} = \frac{r_F}{C_{F(t=0)}} \quad (15)$$

$$k = k_0 e^{-\frac{E_a}{RT}} \quad (16)$$

Temperature (°C)	Time (min)	FFA conversion (%)
150	15	1.68
	30	3.99
	60	5.25
	120	9.68
	180	12.23
	240	19.44
	360	28.39
175	15	10.13
	30	15.36
	60	19.36
	120	24.21
	180	34.74
	240	43.06
	360	37.88
200	15	9.46
	30	17.97
	60	29.41
	120	38.35
	180	45.89
	240	48.53
	360	49.55

Table 5.
 FFA conversion of the esterification reaction kinetic tests.

In these equations,

T = Absolute temperature at which the kinetic test was performed (K).

R = Universal gas constant (J/K.mol).

F = Fatty Acids (FFA).

A = Alcohol (ethanol).

E = Ethyl Esters (FAEE).

W = Water.

C_n = Concentration of compound n (mol/L).

t = time (s).

4.1.2 Process simulation

The compounds defined for the simulation of the fatty acid esterification with ethanol were specified in the Aspen Plus V.12 process simulator, with the fatty acid and oil fraction represented by oleic acid and triolein, respectively. A similar approach was used by other researchers as a simplification of the numerous components of the acid and oil fraction of the feedstock [58–60]. The NRTL thermodynamic model [61] was selected to evaluate the activity coefficients of the components of the reaction mixture and the NRTL binary interaction parameters missing from the simulator database were estimated directly through the Aspen Plus estimation tool that uses the UNIFAC model [62].

The flowsheet developed for the process simulation is shown in **Figure 4** and consists of two columns, the first being responsible for the reactive distillation of the reactants fed to the process (C-EST) and the second for removing approximately 95% of the ethyl esters (FAEE) produced (C-DIST).

The simulated reactive distillation column has 22 total stages, of which 14 compose the reactive zone (5 to 18), while the C-DIST column consists of 10 total stages. The columns operating parameters are presented in **Tables 6** and 7. Both the distillation columns have kettle-type reboilers, however the C-EST column is equipped with a total condenser, while the C-DIST with a partial condenser to separate the ethyl esters from the remaining oil and excess ethanol. It is noteworthy that the liquid phase composition and temperature profile graphs, as well as the conversions obtained follow the data referring to the process after the optimization described later.

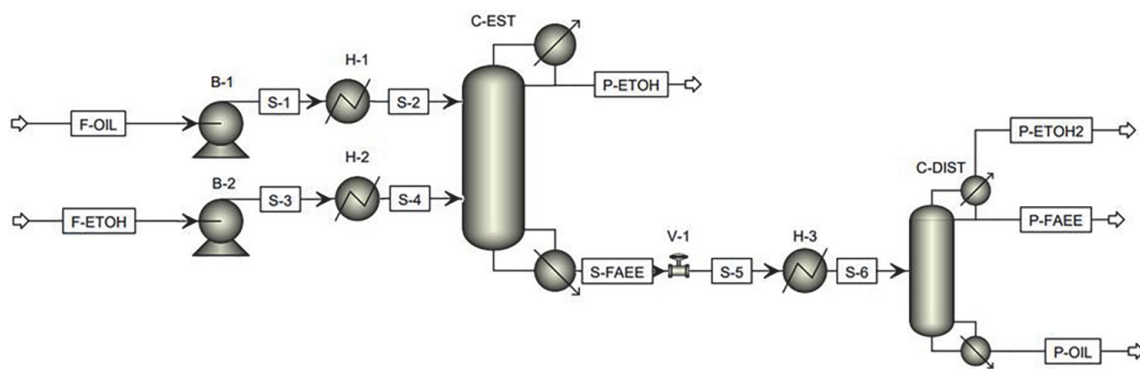


Figure 4.

Flowsheet of the FFA esterification process (F = feed, P = product, S = intermediate stream, H = heat exchanger, B = pump, V = valve, C = column).

Parameters	Before optimization
Stages	22
Oil feed stage	5
Ethanol feed stage	18
Absolute pressure (bar)	4
Distillate: feed molar ratio	0.62
Reflux molar ratio	0.08

Table 6.

Reactive distillation column operating parameters (C-EST).

Parameters	Distillation column
Stages	10
Feed stage	4
Absolute pressure (bar)	0.03
Distillate: feed molar ratio	0.51
Reflux molar ratio	1.5

Table 7.

Distillation column operating parameters (C-DIST).

Stream	F-OIL	F-ETOH
Temperature (°C)	20.00	20.00
Absolute pressure (bar)	1.00	1.00
Enthalpy (kW)	-4058.33	-2461.46
Mass Flow (kg/h)		
Oleic acid (FFA)	900	—
Ethanol	—	1467.86
Triolein	5100	—
Ethyl oleate (FAEE)	—	—
Water	—	—

Table 8.
 Properties of the oil feed and ethanol streams (F-OIL and F-ETOH).

The H-1 and H-2 heat exchangers are responsible for heating the oil (F-OIL) and ethanol (F-ETOH) streams up to 200°C and 50°C, respectively, shown in **Table 8**, while the pumps B-1 and B-2 increase the pressure of the feed streams from 1 bar to 10 bar.

4.1.3 Optimization of the reactive distillation column

The optimization of the process parameters of the esterification reactive distillation column was performed using the MATLAB® R2020b software by implementing the MEIGO package (Metaheuristics for Bioinformatics Global Optimization) [63], an optimization supplement for global optimal search which can be used to optimize industrial processes [64, 65]. The results obtained through Aspen Plus simulations were provided to MATLAB, where the optimization algorithm was performed, and new obtained values of the variables evaluated were used to carry out new simulations iteratively.

The Particle Swarm Optimization (PSO) method was applied to minimize the objective function that describes the conversion of fatty acids (Eq. (17)), starting from an initial population of 50 particles (solution vectors) defined by the algorithm in the pre-defined search intervals.

For the simulation, the varied parameters were molar reflux ratio, internal pressure, molar ratio between distillate stream and total feed, and oil and ethanol feed stages. As restrictions, the reboiler temperature, the recovery of the desired product (ethyl esters) at the bottom of the column and the feed stages of the reagents were evaluated with Eqs. (18)–(20). The reboiler temperature upper limit was defined as 200°C to avoid degradation of the reagents or products and excessive use of the hot utility. It is observed that the minimization of the negative value of the conversion corresponds to the maximization of its positive value.

$$\min(\text{conversion}(\%)) = -\left(1 - \frac{\text{Prod}_{\text{Bot}}}{\text{FFA}_{\text{in}}}\right) \times 100 \quad (17)$$

$$T_{\text{Reb}} \leq 200^\circ\text{C} \quad (18)$$

$$\text{Rec}_{\text{Prod}} = \frac{\text{Prod}_{\text{Bot}}}{\text{Prod}_{\text{Top}} + \text{Prod}_{\text{Bot}}} \geq 0.99 \quad (19)$$

$$FS_{\text{Oil}} \leq FS_{\text{EtOH}} \quad (20)$$

In these equations,

FFA_{in} = Molar flow of fatty acids in the feed stream (kmol/h).

T_{Reb} = Reboiler temperature ($^{\circ}\text{C}$).

Rec_{Prod} = Desired product fraction recovered at the column bottom.

$Prod_{Bot}$ = Molar flow of the desired product at the column bottom (kmol/h).

$Prod_{Top}$ = Molar flow of the desired product at the column top (kmol/h).

FS_{Oil} = Acid oil (corn distillers oil) feed stage.

FS_{EtOH} = Ethanol feed stage.

4.2 Results

4.2.1 Kinetic parameters fitting

The kinetic constants obtained through the discussed methodology are presented in **Table 9**, with the direct reaction of ethyl esters formation indicated by the subscript “1” and the reverse reaction of fatty acids formation indicated by the subscript “2”. **Figure 5** shows the comparison between the experimental and calculated conversions, along with the R^2 coefficient of the fit for each temperature.

Observing the results presented, it is noted that the data fitting at 200°C presented a high coefficient of determination, while the data fitting at 175°C obtained a reduced R^2 . However, as the temperature in the reactive section of the esterification column is, on average, close to 195°C , it was concluded that due to the excellent results achieved in the data fitting at 200°C , the use of the estimated

Parameter	Value
$K_{0,1}(\text{L/mol.s})$	252.786
$K_{0,2}(\text{L/mol.s})$	207.093
$E_{a1}(\text{J/mol})$	51,357.1
$E_{a2}(\text{J/mol})$	39,244.1

Table 9.
Estimated kinetic constants for the esterification reaction.

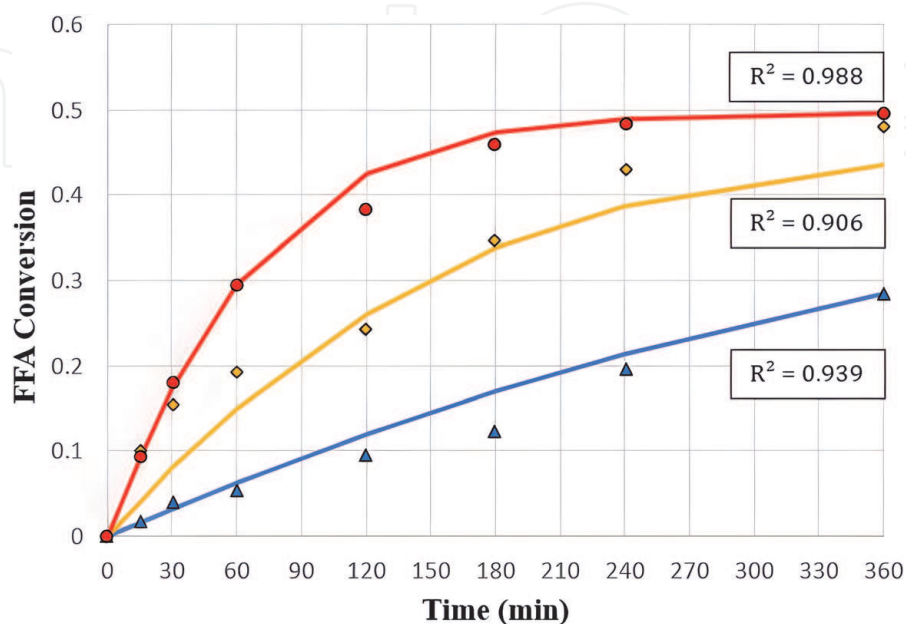


Figure 5.
Experimental (—) and calculated FFA conversion at 150°C (Δ), 175°C (\diamond) and 200°C (\circ).

kinetic parameters would not hinder the development of a simulation faithful to the real behavior of the reaction.

4.2.2 Esterification of fatty acids

The composition and temperature profiles along the stages of the reactive distillation column (column C-EST in **Figure 4**) are presented in **Figures 6** and **7**.

The liquid phase composition profile of the C-EST column (**Figure 6**) indicates that the major component for all stages with values higher than 5 (closer to the bottom) is triolein, while in the others there is a predominance of oleic acid, ethyl oleate (FAEE), ethanol and water, since only negligible amounts of triolein are evaporated along the column, as seen in the vapor phase mass composition profile. Additionally, there is a significant increase in the fraction of ethanol and water in the liquid state in the first stage due to the use of a total condenser in the reactive distillation column.

The composition of the streams that characterize the main products of the process (S-FAEE, P-OIL and P-FAEE) are presented in **Table 10** and, based on the simulation results, there is a final fatty acids conversion (mol) of 83.97% inside the

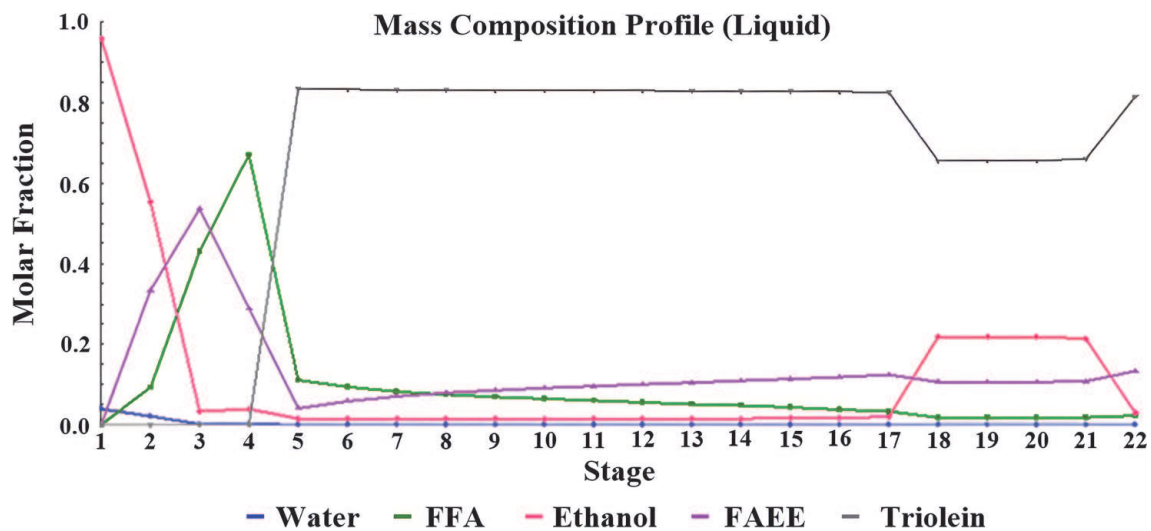


Figure 6.
Liquid phase mass composition profile (C-EST).

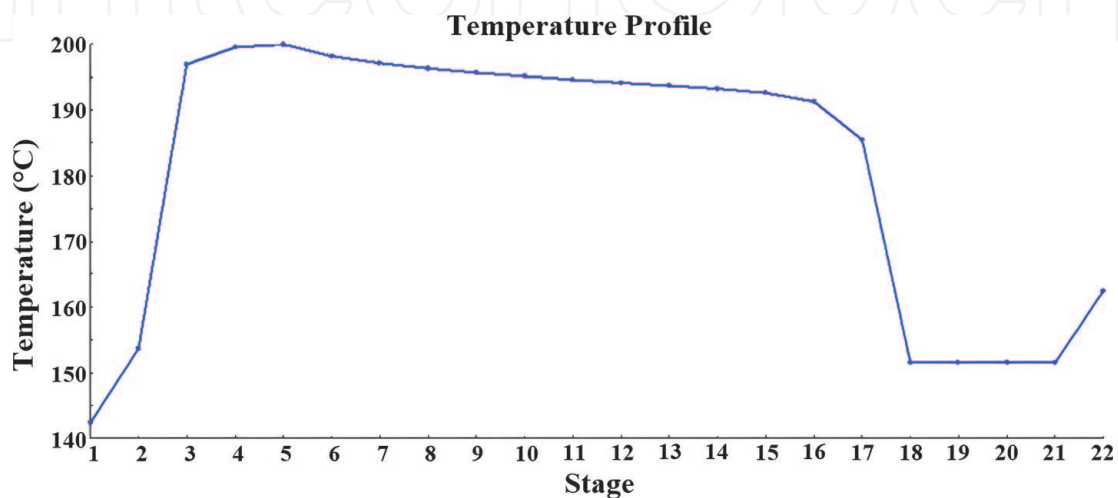


Figure 7.
Column temperature profile (C-EST).

Stream	S-FAEE	P-FAEE	P-OIL
Temperature (°C)	162.39	90.00	305.08
Absolute pressure (bar)	8.13	0.03	0.03
Enthalpy (kW)	-3813.85	-506.62	-2532.30
Mass Flow (kg/h)			
Oleic acid (FFA)	144.22	11.80	132.41
Ethanol	186.96	0.58	—
Triolein	5100.00	—	5100.00
Ethyl oleate (FAEE)	830.34	780.97	48.43
Water	0.58	—	—

Table 10.
Composition of the main product streams.

Equipment	Energy demand (kW)
H-1	619.71
H-2	31.60
C-EST (condenser)	-295.57
C-EST (reboiler)	330.86
C-DIST (condenser)	-581.94
C-DIST (reboiler)	1095.36

Table 11.
Energy demand of the process equipment.

column, 94.00% of which is recovered in the P-FAEE stream, while 5.83% is recovered in the P-OIL stream. The remaining 0.17% of FAEE is located at the P-ETOH2 stream. The resulting stream of the desired product (P-FAEE) has a purity (FAEE) greater than 98%, resulting in an ester content superior to the value described in Brazilian and European specifications [66, 67].

In **Table 10**, it is possible to observe that there are still traces of ethyl esters present in the oil stream. However, this amount corresponds to less than 1% of the total mass fraction of the stream. P-OIL, therefore, was considered to be non-significant. Furthermore, of the 900 kg/h of FFA fed to the process, only 132.41 kg/h remain, characterizing a reduction of 85.29% of the total fatty acid mass. Finally, the energy demands for H-1, H-2, condensers and reboilers of columns C-EST and C-DIST are presented in **Table 11**.

4.2.3 Optimization of the reactive distillation column

Table 12 shows the limits and initial estimates for the variables evaluated for the optimization of the esterification process. **Table 13** displays the constraints imposed on the reboiler temperature, ethyl ester recovery fraction (FAEE), and conversion. The values chosen as initial estimates were obtained by manually setting different values for the reflux molar ratio, condenser pressure, and distillate feed molar ratio, and adopting the best result obtained.

The results obtained are shown in **Figure 8**, with a maximum conversion of 83.97% and the final values of the variables are added to **Table 14**.

Variable	Molar reflux ratio	Condenser pressure (bar)	Distilled molar ratio: feed	Oil feed stage	Ethanol feed stage
Lower Limit	0.005	0.01	0.50	5	5
Upper Limit	2	10	0.70	18	18
Initial Estimate	0.08	4	0.62	5	18

Table 12.

Lower, upper limits and initial estimates for the variables evaluated in the esterification reaction optimization process.

Restrictions	Reboiler temperature (°C)	Recovery fraction of FAEE	Conversion (%)
Lower Limit	-273.15	0.99	0
Upper Limit	200	1.00	100

Table 13.

Initial constraints for the response variables for the variables evaluated in the esterification reaction optimization process.

An additional simulation performed in a CSTR reactor achieved an FFA conversion of 51.06%, while the maximum average conversion in the kinetic tests (200°C) was 49.55%. The simulated CSTR operated at a constant temperature of 200°C with the residence time of 3 h (same duration of the experimental tests) and was fed with streams following equal mass flows and compositions to the RDC column feed streams. Thus, the optimization results represent a significant improvement of 64.45% and 69.46% compared to the CSTR and experimental tests, respectively, inferring that the use of a reactive distillation column could be beneficial to the process.

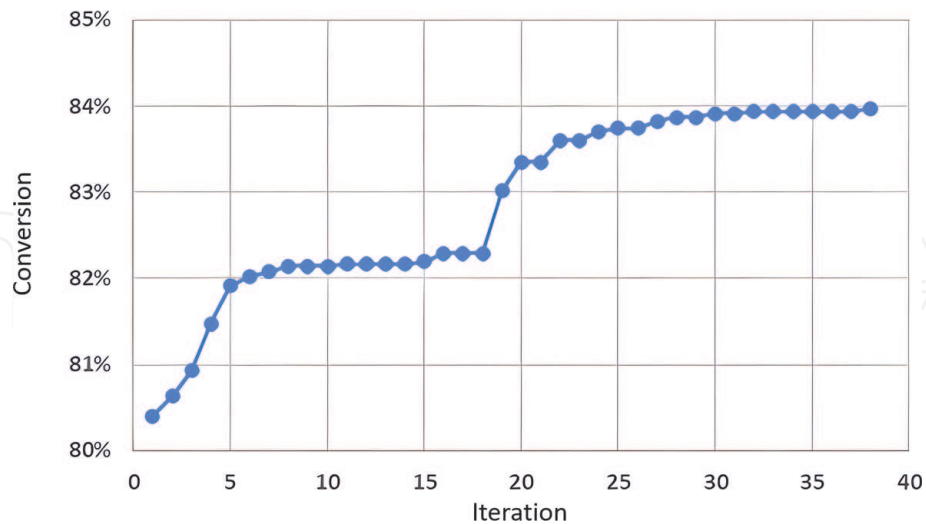


Figure 8.

Evolution of the FFA conversion as a function of the number of optimization iterations.

Variable	Molar reflux ratio	Condenser pressure (bar)	Distilled molar ratio: feed	Oil feed stage	Ethanol feed stage
Result	0.1130	8.1314	0.6806	5	18

Table 14.

Response vector of input variables for the esterification reaction optimization process.

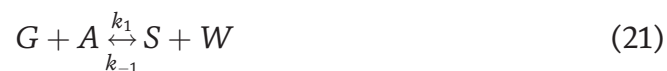
5. Solketal production simulation

5.1 Justification

As biodiesel production increases so do the production of glycerol as for each liter of biodiesel produced, approximately 100 mL of crude glycerol are obtained [68]. Among the transformation processes for glycerol to viable chemical intermediates, glycerol ketalization for the production of solketal has gained prominence. Solketal can be used as an additive to increase the octane and fluid dynamic properties of the fuel. The addition of up to 5% by volume of solketal to gasoline leads to a significant decrease in gum formation [69]. With this motivation, this study aims to simulate the operation of a reactive distillation column for the production of solketal from glycerol with acetone using heterogeneous catalysis, with high conversion of reagents and separation of the components of the reaction.

5.2 Methodology

The applied methodology considers the ketalization reaction of glycerol (G) with acetone (A), forming solketal (S) and water (W). The reaction is considered reversible and elementary, being described by Eq. (21):



A pseudo-homogeneous model was used to describe the reaction kinetics through a system of differential equations of concentration over time, at different temperatures, in which the kinetic constants of the direct and inverse reaction are represented, respectively, by k_1 and k_{-1} (L/mol.s), while the molar concentrations (mol/L) of the species involved are given by C_G , C_A , C_S and C_W (Eq. (22)).

$$-r_G = k_1 C_G C_A - k_{-1} C_S C_W \quad (22)$$

The solution of the system of differential equations using a 4th order Runge Kutta method [57] and the fitting of the kinetic parameters, k_1 and k_{-1} , and subsequent estimation of the Arrhenius equation parameters were performed by a Nelder–Mead simplex algorithm [56]. The experimental data used was retrieved from the study of [70].

The kinetic parameters evaluated were later used to predict the solketal formation reaction in a reactive distillation column, using the rigorous RADFRAC distillation model of the Aspen Plus commercial simulation software. The system considered in this study is shown in **Figure 9**.

Using the estimated kinetic parameters, the glycerol ketalization reaction for the production of solketal was modeled in the Aspen Plus software. For the process simulation, the pressure inside the column was set at 10 atm. The feeding of the 13-stage column, RDC in **Figure 9**, are streams GLI-02 and ACE-02, originated from the heating of the currents GLI-01 and ACE-01 up to 95°C and 55°C, by the heat exchangers H1 and H2, respectively.

The ACE-01 stream is composed only of acetone, while GLI-01 contains 80% glycerol and 20% water by mass, disregarding other components such as methanol or dissolved salts normally present in glycerol from biodiesel production processes [71]. The products of reactive distillation are characterized by TOP-P and BOT-P streams, which correspond, respectively, to the streams rich in the most volatile and least volatile substances in the process.

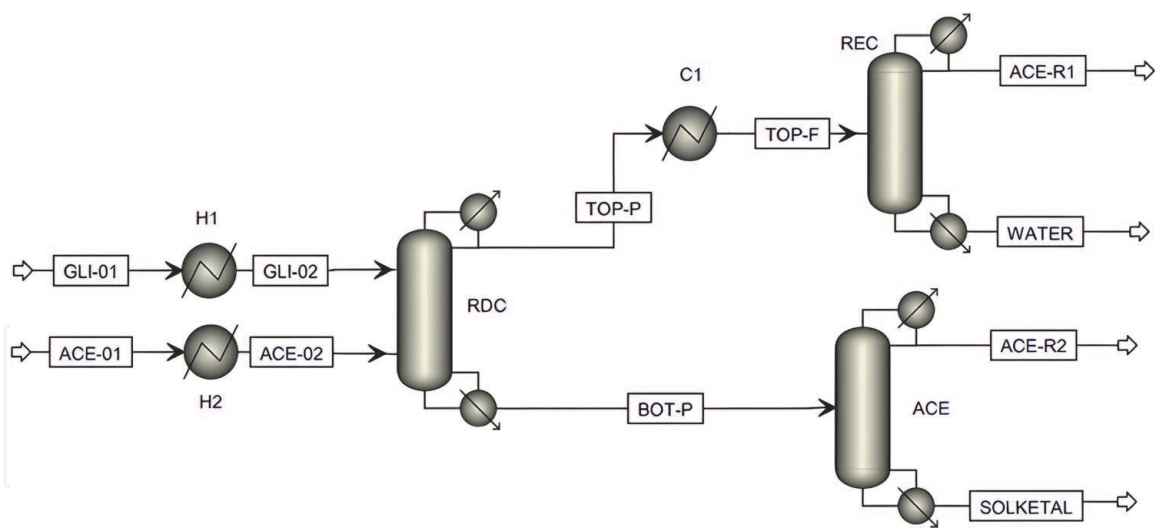


Figure 9.
 Flowsheet of the solketal production process used in this study.

5.3 Results

Figure 10 shows the concentrations as a function of time according to the fitted kinetic parameters data.

Analyzing **Figure 10**, it is observed that the curves generated using the fitted parameters represented the experimental data satisfactorily. **Table 15** presents the process specifications obtained after a sensitivity analysis, aiming to simulate a column with optimal operating conditions. **Figure 11** shows the composition profile in the liquid phase as a function of the column stage number (1 = condenser and 13 = reboiler).

The conversion of glycerol obtained for the operational conditions defined for the simulation was 98.2%, indicating the reaction occurred inside the column.

The SOLKETAL stream in **Figure 9** has 99.53% solketal and the WATER stream consists of 99.82% water, on a mass basis. Thus, the simulations show that the

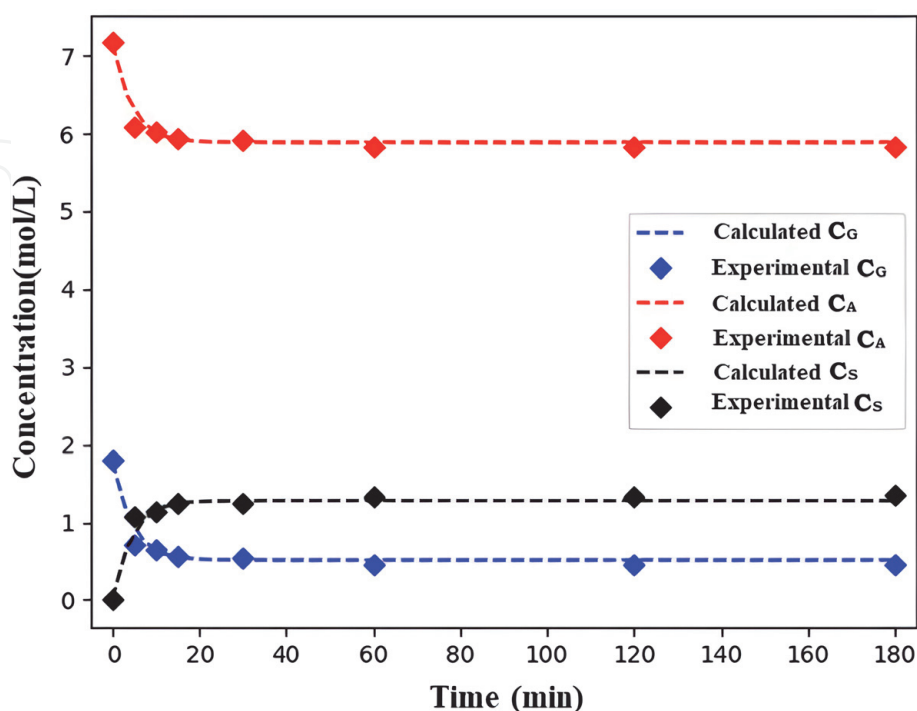


Figure 10.
 Experimental and calculated concentrations (80°C).

Parameter	Description
Number of stages	13
Condenser type	Total
Reboiler type	Kettle
Molar reflux ratio	0.69
Reboiler/condenser heat duty	55.000 / -43.723 cal/s
Column pressure	10 bar
Glycerol feed	3rd stage
Acetone feed	11th stage
Feed properties	95 and 55°C - 1 bar
Glycerol feed molar flow	2.500 kmol/h
Water feed molar flow	0.625 kmol/h
Acetone feed molar flow	15.000 kmol/h
Ketalization reaction stages	3 to 11

Table 15.
RDC column specifications.

methodology employed results in a high purity solketal product stream with solketal conversion superior to 98%. However, additional studies are needed to assess the effect of possible intermediate reactions on the process yield.

6. Conclusions

In this chapter, a general introduction regarding reactive distillation technology and its application to the biodiesel production process was presented. A literature-based mathematical model to describe reactive distillation columns was discussed, along with experimental and simulation studies developed by the authors of this chapter, using commercial software such as Aspen Plus.

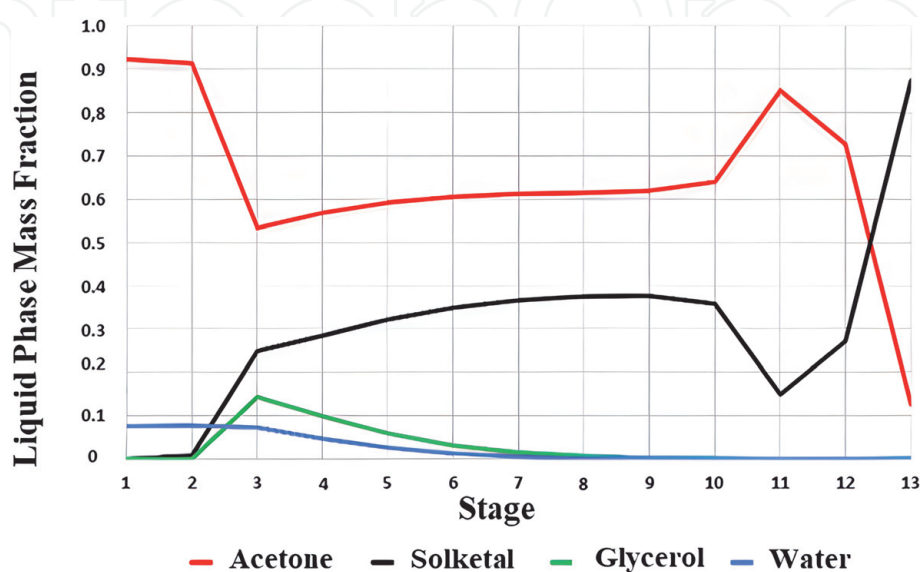


Figure 11.
RDC column liquid phase composition profile.

In the case study of biodiesel production through the esterification of a low-cost feedstock, the application of an optimized reactive distillation column promoted an improvement of approximately 70% about FFA conversion. The resulting product stream attained purity above 98% in relation to alkyl esters. Additionally, the production of solketal aiming at the valorization of a co-product of the biodiesel production process (glycerol), was studied through the development of a flowsheet in the Aspen Plus simulator, resulting in a solketal stream with purity above 99%.

The results obtained through the developed studies indicate that the reactive distillation technology, applied to fatty acid esterification reactions for the production of biodiesel and ketalization of glycerol for the production of solketal, is promising and attractive in technical terms, however, further studies are necessary to analyze the economic feasibility of both processes.

Acknowledgements

The authors thank UTFPR and Sinochem Petroleum Brazil Limited (project 001/2019) for financial support.

Author details

Guilherme Machado^{1*}, Marcelo Castier², Monique dos Santos³, Fábio Nishiyama¹, Donato Aranda⁴, Lúcio Cardozo-Filho⁵, Vladimir Cabral⁵ and Vilmar Steffen⁶

1 Federal Technological University of Paraná, Londrina, Brazil

2 German Paraguayan University, San Lorenzo, Paraguay

3 Sinochem Petroleum Brazil Limited, Rio de Janeiro, Brazil


4 Federal University of Rio de Janeiro, Rio de Janeiro, Brazil

5 State University of Maringá, Maringá, Brazil

6 Federal Technological University of Paraná, Francisco Beltrão, Brazil

*Address all correspondence to: guilhermed@utfpr.edu.br

IntechOpen

© 2022 The Author(s). Licensee IntechOpen. This chapter is distributed under the terms of the Creative Commons Attribution License (<http://creativecommons.org/licenses/by/3.0>), which permits unrestricted use, distribution, and reproduction in any medium, provided the original work is properly cited. 

References

- [1] Gotze L, Bailer O, Moritz P, von Scala C. Reactive distillation with KATAPAK®. *Catalysis Today*. 2001;**69**: 201-208. DOI: 10.1016/S0920-5861(01)00370-4
- [2] Machado GD. Simulação computacional da produção de biodiesel por hidroesterificação [thesis]. Maringá: Universidade Estadual de Maringá; 2011
- [3] Taylor R, Krishna R. Modelling reactive distillation. *Chemical Engineering Science*. 2000;**55**:5183-5229. DOI: 10.1016/S0009-2509(00)00120-2
- [4] Noeres C, Kenig EY, Górak A. Modelling of reactive separation processes: Reactive absorption and reactive distillation. *Chemical Engineering and Processing*. 2003;**42**: 157-178. DOI: 10.1016/S0255-2701(02)00086-7
- [5] Segovia-Hernández JG, Hernández S, Petriciolet AB. Reactive distillation: A review of optimal design using deterministic and stochastic techniques. *Chemical Engineering and Processing*. 2015;**97**:134-143. DOI: 10.1016/j.cep.2015.09.004
- [6] Simasatikul L, Arpornwichanop A. Economic evaluation of biodiesel production from palm fatty acid distillate using a reactive distillation. *Energy Procedia*. 2017;**105**:237-243. DOI: 10.1016/j.egypro.2017.03.308
- [7] Haydary J. *Chemical Process Design and Simulation: Aspen Plus and Aspen Hysys Applications*. 1st ed. Hoboken: John Wiley & Sons; 2019
- [8] Backhaus AA. Apparatus for the manufacture of esters. US1400850 (Patent), 1921
- [9] Backhaus AA. Apparatus for the production of esters. US1400851 (Patent), 1921
- [10] Backhaus AA. Method for the production of esters. US1400852 (Patent), 1921
- [11] Malone MF, Doherty MF. Reactive distillation. *Industrial & Engineering Chemistry Research*. 2000;**39**:3953-3957
- [12] Agreda VH, Partin LR. Reactive distillation process for the production of methyl acetate. US4435595 (Patent), 1984
- [13] Stankiewicz A, Moulijn J. Process intensification: Transforming chemical engineering. *Industrial & Engineering Chemistry Research*. 2002;**41**:1920-1924
- [14] Sander S, Zuber L. Reactive distillation process and plant for obtaining acetic acid and alcohol from the hydrolysis of methyl acetate EP2502655A1 (Patent). 2012
- [15] Panchal CB, Prindle JC. Method of producing high-concentration alkyl carbonates using carbon dioxide as feedstock. US9796656 (Patent). 2017
- [16] Pacheco N, Dorato M, Jacquin M, Dastillung R, Couderc S. Method for producing butadiene from butanediols. WO2017102743A1 (Patent). 2017
- [17] Gadewar SB, Vicente BC, Stoimenov PK. Production of butyl acetate from ethanol. US20160297737A1 (Patent). 2016
- [18] Hoyme CA, Holcombe EF. Reactive distillation process for hydrolysis of esters. US6518465B2 (Patent). 2001
- [19] Kronemayer H, Dahlhoff E, Lanver A. Process for preparing carboxylic esters by reactive distillation. WO2011131643A2 (Patent). 2011
- [20] Almeida-Rivera CP. Designing Reactive Distillation Processes with

Improved Efficiency [Thesis]. Delft: Universidade Técnica de Delft; 2005

[21] Noeres C, Kening EY, Gorak A. Modelling of reactive separation processes: Reactive absorption and reactive distillation. *Chemical Engineering and Processing*. 2003;**42**: 157-178. DOI: 10.1016/S0255-2701(02)00086-7

[22] Kularathne IW, Gunathilake CA, Rathneweera AC, Kalpage CS, Rajapakse S. The effect of use of biodiesel on environmental pollution – A review. *International Journal of Renewable Energy Research*. 2019;**9**:3

[23] Bhatia SK, Bhatia RK, Jeon J, Pugazhendhi A, Awasthi MK, Kumar D, et al. An overview on advancements in biobased transesterification methods for biodiesel production: Oil resources, extraction, biocatalysts and process intensification technologies. *Fuel*. 2021; **285**:1-20. DOI: 10.1016/j.fuel.2020.119117

[24] Atadashi IM, Aroua MK, Aziz AA. Biodiesel separation and purification: A review. *Renewable Energy*. 2011;**36**: 437-443. DOI: 10.1016/j.renene.2010.07.019

[25] Aranda DAG, Gonçalves JA, Peres JS, Ramos ALD, Melo CAR Jr, Antunes OAC, et al. The use of acids, niobium oxide, and zeolite catalysts for esterification reactions. *Journal of Physical Organic Chemistry*. 2009;**22**: 709-716. DOI: 10.1002/poc.1520

[26] Freedman B, Pryde EH, Mounts TL. Variables affecting the yields of fatty esters from transesterified vegetable oils. *Journal of the American Oil Chemists' Society*. 1984;**61**:1638-1643

[27] Hajjari M, Tabatabaei M, Aghbashlo M, Ghanavati H. A review on the prospects of sustainable biodiesel production: A global scenario with an emphasis on waste-oil biodiesel

utilization. *Renewable and Sustainable Energy Reviews*. 2017;**72**:445-464. DOI: 10.1016/j.rser.2017.01.034

[28] Gao X, Zhao R, Cong H, Na J, Shi Y, Li H, et al. Reactive distillation toward an ecoefficient process of biodiesel manufacture from waste oil: Pilot-scale experiments and process design. *Industrial & Engineering Chemistry Research*. 2020;**59**:14935-14946. DOI: 10.1021/acs.iecr.0c02343

[29] Haq IU, Akram A, Nawaz A, Zohu X, Abbas SZ, Xu Y, et al. Comparative analysis of various waste cooking oils for esterification and transesterification processes to produce biodiesel. *Green Chemistry Letters and Reviews*. 2021;**14**:461-472. DOI: 10.1080/17518253.2021.1941305

[30] Ding J, Xia Z, Lu J. Esterification and deacidification of a waste cooking oil (TAN 68.81 mg KOH/g) for biodiesel production. *Energies*. 2012;**5**:2683-2691. DOI: 10.3390/en5082683

[31] López-Ramírez MD, García-Ventura UM, Barroso-Munoz FM, Segovia-Hernández FO, Hernández S. Production of methyl oleate in reactive separation systems. *Chemical Engineering and Technology*. 2016;**39**: 271-275. DOI: 10.1002/ceat.201500423

[32] Kiss AA, Omota F, Dimian AC, Rothenberg G. The heterogeneous advantage: Biodiesel by catalytic reactive distillation. *Topics in Catalysis*. 2006;**40**:1-4. DOI: 10.1007/s11244-006-0116-4

[33] Kiss AA, Dimian AC, Rothenberg G. Biodiesel by catalytic reactive distillation powered by metal oxides. *Energy & Fuels*. 2008;**22**:598-604. DOI: 10.1021/ef700265y

[34] Kusumaningtyas RD, Prasetiawan H, Pratama BR, Prasetya D, Hisyam A. Esterification of non-edible oil mixture in reactive distillation

column over solid acid catalyst: Experimental and simulation study. *Journal of Physical Science*. 2018;**29**: 215-226. DOI: 10.21315/jps2018.29.s2.17

[35] Ali SS, Asif M, Basu A. Design and simulation of high purity biodiesel reactive distillation process. *Polish Journal of Chemical Technology*. 2019; **21**:1-7. DOI: 10.2478/pjct-2019-0022

[36] Banchemo M, Gozzelino G. Nb2O5-catalyzed kinetics of fatty acids esterification for reactive distillation process simulation. *Chemical Engineering Research and Design*. 2015; **100**:292-301. DOI: 10.1016/j.cherd.2015.05.043

[37] Cossio-Vargas E, Hernandez S. Segobia-Hernandez, Cano-Rodriguez MI. Simulation study of the production of biodiesel using feedstock mixtures of fatty acids in complex reactive distillation columns. *Energy* 2011;**36**: 6289-6297. 10.1016/j.energy.2011.10.005

[38] Machado GD, Aranda DAG, Castier M, Cabral VF, Cardozo-Filho L. Computer simulation of fatty acids esterification in reactive distillation columns. *Industrial & Engineering Chemistry Research* 2011;**50**: 10176-10184. [https:// dx.doi.org/10.1021/ie102327y](https://dx.doi.org/10.1021/ie102327y)

[39] Machado GD, Pessoa FLP, Castier M, Aranda DAG, Cabral VF, Cardozo-Filho L. Biodiesel production by esterification of hydrolyzed soybean oil with ethanol in reactive distillation columns: Simulation studies. *Industrial & Engineering Chemistry Research* 2013;**52**:9461-9469. [https:// dx.doi.org/10.1021/ie400806q](https://dx.doi.org/10.1021/ie400806q)

[40] Margarida BR, Flores LI, Hamerski F, Voll FAP, Luz Jr LFL. Simulation, optimization and economic analysis of process to obtain esters from fatty acids. *Biofuels, Bioproducts &*

Biorefining. 2021;**15**:749-769. DOI: 10.1002/bbb.2186

[41] da Silva NL, Santander CMG, Batistella CB, Filho RM, Maciel MRW. Biodiesel production from integration between reaction and separation system: Reactive distillation process. *Applied Biochemistry and Biotechnology*. 2010; **161**:245-254. DOI: 10.1007/s12010-009-8882-7

[42] He BB, Singh AP, Thompson JC. Experimental optimization of a continuous-flow reactive distillation reactor for biodiesel production. *Transactions of ASAE*. 2005;**48**: 2237-2243. DOI: 10.13031/2013.20071

[43] He BB, Singh AP, Thompson JC. A novel continuous-flow reactor using reactive distillation for biodiesel production. *Transactions of the ASABE*. 2006;**49**:107-112. DOI: 10.13031/2013.20218

[44] Noshadi I, Amin NAS, Parnas RS. Continuous production of biodiesel from waste cooking oil in a reactive distillation column catalyzed by solid heteropolyacid: Optimization using response surface methodology (RSM). *Fuel*. 2012;**94**:156-164. DOI: 10.1016/j.fuel.2011.10.018

[45] Prasertsit K, Mueanmas C, Tongurai C. Transesterification of palm oil with methanol in a reactive distillation column. *Chemical Engineering and Processing*. 2013;**70**: 21-26. DOI: 10.1016/j.cep.2013.05.011

[46] Agarwal M, Singh K, Chaurasia SP. Simulation and sensitivity analysis for biodiesel production in a reactive distillation column. *Polish Journal of Chemical Technology*. 2012;**14**:59-65. DOI: 10.2478/v10026-012-0085-2

[47] Simasatikul L, Siricharnsakunchai P, Patcharavorachot Y, Assabumrungrat S, Arpornwichanop A. Reactive distillation for biodiesel production

from soybean oil. *Korean Journal of Chemical Engineering*. 2011;**28**: 649-655. DOI: 10.1007/s11814-010-0440-z

[48] Mondal B, Jana AK. Techno-economic feasibility of reactive distillation for biodiesel production from algal oil: Comparing with a conventional multiunit system. *Industrial & Engineering Chemistry Research*. 2019;**58**: 12028-12040. DOI: 10.1021/acs.iecr.9b00347

[49] Boon-Anuwat KW, Aiouache F, Assabumrungrat S. Process design of continuous biodiesel production by reactive distillation: Comparison between homogeneous and heterogeneous catalysts. *Chemical Engineering and Processing*. 2015;**92**: 33-44. DOI: 10.1016/j.cep.2015.03.025

[50] Poddar T, Jagannath A, Almansoori A. Biodiesel production using reactive distillation: A comparative simulation study. *Energy Procedia*. 2015;**75**:17-22. DOI: 10.1016/j.egypro.2015.07.129

[51] Alfradique MF, Castier M. Automatic generation of procedures for the simulation of reactive distillation using computer algebra. *Computers & Chemical Engineering*. 2005;**29**: 1875-1884. DOI: 10.1016/j.compchemeng.2005.04.002

[52] Chen F, Huss RS, Malone MF, Doherty MF. Simulation of kinetic effects in reactive distillation. *Computers & Chemical Engineering*. 2000;**24**:2457-2472. DOI: 10.1016/S0098-1354(00)00609-8

[53] Machado GD, de Souza TL, Aranda DAG, Pessoa FLP, Castier M, Cabral VF, et al. Computer simulation of biodiesel production by hydro-esterification. *Chemical Engineering and Processing*. 2016;**103**:37-45. DOI: 10.1016/j.cep.2015.10.015

[54] Gautam P, Singh PP, Mishra A, Singh A, Das SN, Suresh S. Simulation of reactive distillation column. *International Journal of ChemTech Research*. 2013;**5**:1024-1029

[55] Popken T, Steinigeweg S, Gmehling J. Synthesis and hydrolysis of methyl acetate by reactive distillation using structured catalytic packings: Experiments and simulation. *Industrial & Engineering Chemistry Research*. 2001;**40**:1566-1574. DOI: 10.1021/ie0007419

[56] Nelder J, Mead R. A simplex method for function minimization. *The Computer Journal*. 1965;**7**:308-313. DOI: 10.1093/comjnl/7.4.308

[57] Dormand JR, Prince PJ. A family of embedded Runge-Kutta formulae. *Journal of Computational and Applied Mathematics*. 1980;**6**:19-26. DOI: 10.1016/0771-050X(80)90013-3

[58] Hussain Z, Kumar R. Esterification of free fatty acids: Experiments, kinetic modeling, simulation & optimization. *International Journal of Green Energy*. 2018;**15**:629-640. DOI: 10.1080/15435075.2018.1525736

[59] Margarida BR, Flores LI, Hamerski F, Voll FAP, Luz Jr LFL. Simulation, optimization, and economic analysis of process to obtain esters from fatty acids. *Biofuels, Bioproducts and Biorefining*. 2021;**15**:749-769. DOI: 10.1002/bbb.2186

[60] Anene RC, Giwa A. Modelling, simulation and sensitivity analysis of a fatty acid methyl ester reactive distillation process using Aspen plus. *International Journal of Engineering Research in Africa*. 2016;**27**:36-50. DOI: 10.4028/www.scientific.net/JERA.27.36

[61] Renon H, Prausnitz JM. Local compositions in thermodynamic excess functions for liquid mixtures. *AIChE*

- Journal. 1968;**14**:135-144. DOI: 10.1002/aic.690140124
- [62] Fredenslund A, Jones RL, Prausnitz JM. Group-contribution estimation of activity coefficients in nonideal liquid mixtures. *AICHE Journal*. 1975;**21**:1086-1099. DOI: 10.1002/aic.690210607
- [63] Egea JA, Henriques D, Cokelaer T, Villaverde AF, Macnamara A, Danciu DP, et al. MEIGO: An open-source software suite based on metaheuristics for global optimization in systems biology and bioinformatics. *BMC Bioinformatics*. 2014;**15**:1-9. DOI: 10.1186/1471-2105-15-136
- [64] Bonfim-Rocha L, Gimenes ML, Farias SHB, Silva RO, Esteller LJ. Multi-objective design of a new sustainable scenario for bio-methanol production in Brazil. *Journal of Cleaner Production*. 2018;**187**:1043-1056. DOI: 10.1016/j.jclepro.2018.03.267
- [65] Luna R, López F, Pérez-Correa JR. Minimizing methanol content in experimental Charentais alembic distillations. *Journal of Industrial and Engineering Chemistry*. 2018;**57**:160-170. DOI: 10.1016/j.jiec.2017.08.018
- [66] Ministério de Minas e Energia. Especificação do Biodiesel [Internet]. 2020. Available from: <https://www.gov.br/anp/pt-br/assuntos/producao-e-fornecimento-de-biocombustiveis/biodiesel/especificacao-do-biodiesel> [Accessed: 2021-10-04]
- [67] Sajjadi B, Raman AA, Arandiyani H. A comprehensive review on properties of edible and non-edible vegetable oil-based biodiesel: Composition, specifications and prediction models. *Renewable and Sustainable Energy Reviews*. 2016;**63**:62-92. DOI: 10.1016/j.rser.2016.05.035
- [68] Mota CJA, Pinto BP. Transformações catalíticas do glicerol para inovação na indústria química. *Revista Virtual de Química*. 2017;**9**:135-149. DOI: 10.21577/1984-6835.20170011
- [69] Mota CJA, Rosenbach N Jr, Costa J, Silva F. Glycerin derivatives as fuel additives: The addition of glycerol/acetone ketal (solketal) in gasolines. *Energy & Fuels*. 2010;**24**:2733-2736. DOI: 10.1021/ef9015735
- [70] Rossa V, Pessanha YSP, Diaz GC, Camara LDT, Pergher SBC, Aranda DAG. Reaction kinetic study of solketal production from glycerol ketalization with acetone. *Industrial & Engineering Chemistry Research*. 2016;**54**:479-488. DOI: 10.1021/acs.iecr.6b03581
- [71] Mota CJA, Silva CXX, Gonçalves VLC. Gliceroquímica: novos produtos e processos a partir da glicerina de produção de biodiesel. *Química Nova*. 2009;**32**:639-648. DOI: 10.1590/S0100-40422009000300008